Flow and Heat Transfer Due to a Buoyant Ceiling Jet Turning Downward at a Corner

K. Kapoor

Y. Jaluria
Fellow ASME

Department of Mechanical and Aerospace Engineering, Rutgers—The State University of New Jersey, New Brunswick, NJ 08903

An experimental investigation has been carried out on the flow and heat transfer characteristics of a horizontal buoyant ceiling jet that turns downward at a corner to yield a vertical negatively buoyant wall flow. Such flow situations are frequently encountered in thermal energy storage, in electronic systems, and in room fires. However, not much work has been done to understand the basic mechanisms governing such flows, particularly the flow near the corner. In this study, a two-dimensional jet of heated air is discharged adjacent to the lower surface of an isothermal horizontal plate. An isothermal vertical plate is attached at the other end of the horizontal surface, making a right angle corner. The vertical penetration distance of the resulting downward flow is measured and is related to the inflow conditions, particularly to the temperature and velocity at the jet discharge. This penetration distance is found to increase as the distance between the discharge location and the corner is reduced and also as the relative buoyancy level in the inlet flow is decreased. Velocity and temperature measurements are also carried out over the flow region. These indicate that the ceiling flow separates from the horizontal surface just before reaching the corner and then reattaches itself to the vertical wall at a finite distance vertically below the corner. The local surface heat flux measurements show a minimum in the heat transfer rate before the turn, along with a recovery in the heat transfer rate after the turn and the existence of a small recirculation zone near the corner. The net entrainment into the flow and heat transfer rate to the solid boundaries are also measured and correlated with the jet discharge conditions.

Introduction

Buoyant jets are important in meteorological, oceanographic, and environmental studies. Heat rejection to the atmosphere and to water bodies involves turbulent buoyant jets. Solar energy heat extraction and energy storage systems are also concerned with buoyant jet flows. Similarly, a fire in an enclosure generates a fire plume, which impinges on the ceiling and gives rise to a ceiling jet. This ceiling jet spreads outward from the point of impingement and turns downward at the corners of the room. This generates a downward wall flow with an opposing buoyancy force, since this force is directed upward. Although the vertical buoyant jet and ceiling jet have been considered separately, very little work has been done on negatively buoyant wall flows and on the flow characteristics of a downward-turning buoyant ceiling jet. In the present paper, an experimental investigation is reported on such mixed convection flows and the effect of buoyancy on the transport.

Laminar buoyant jets have been studied by several investigators, as reviewed by Jaluria (1986). Turbulent jets, which are of much greater practical interest, have been studied more extensively; see, for instance, Morton (1959), Chen and Rodi (1979), Turner (1979) and List (1982). Jets with opposing buoyancy have been considered by Turner (1966), Seban et al. (1978), and Baines et al. (1990). Goldman and Jaluria (1986) carried out a detailed experimental investigation of negatively buoyant jets. The flow characteristics of a two-dimensional wall jet, with opposing buoyancy force, in an isothermal medium were studied. It was found that the penetration distance δ_p decreases with an increase in the Richardson number Ri, which indicates the relative buoyancy level. The net entrainment into the flow was found to increase with Ri over the investigated range. Jaluria and Kapoor (1988) extended this range and found that large flow rates are generated in the wall flow due to entrainment.

Kapoor and Jaluria (1989) investigated the heat transfer characteristics of a two-dimensional negatively buoyant wall jet in an isothermal environment. The heat transfer rate to an isothermal surface was measured and was found to decrease with an increase in Ri, mainly because of the reduction in the penetration distance, which reduces the heat transfer area. It was also found that the penetration distance decreases with an increase in the wall temperature. This is due to a decrease in the heat transfer, since an increase in surface temperature reduces the temperature difference between the jet inlet and the surface. This, in turn, results in a higher opposing local buoyancy level in the flow and thus a smaller penetration distance.

The transport in a horizontal buoyant ceiling jet has been considered by a few investigators. The flow generated by a ceiling jet, which is driven by the fire plume, has been studied by Alpert (1975). The characteristics of a ceiling jet were investigated by Cooper (1982, 1989). He developed analytical estimates to predict the depth of penetration and entrainment into negatively buoyant, ceiling jet-driven wall flows at the early stages of the fire. You (1985) measured steady-state velocity and temperature profiles in the ceiling jet. Veldman et al. (1975) and Motevalli and Marks (1990) measured the temperature and velocity profiles in ceiling jets driven by a fire plume impinging on a ceiling for different thermal conditions. Baines and Turner (1969) studied the turbulent convection from a source in an enclosed space, simulating the physical circumstance outlined above and indicating different flow regimes that arise.

It is seen from this review of the relevant literature that, although separate studies on vertical and ceiling jets are available, no detailed effort has been directed at the flow and

Contributed by the Heat Transfer Division for publication in the JOURNAL OF HEAT TRANSFER. Manuscript received by the Heat Transfer Division March 1995; revision received August 1995. Keywords: Fire/Flames, Jets, Mixed Convection. Associate Technical Editor: R. Viskanta.

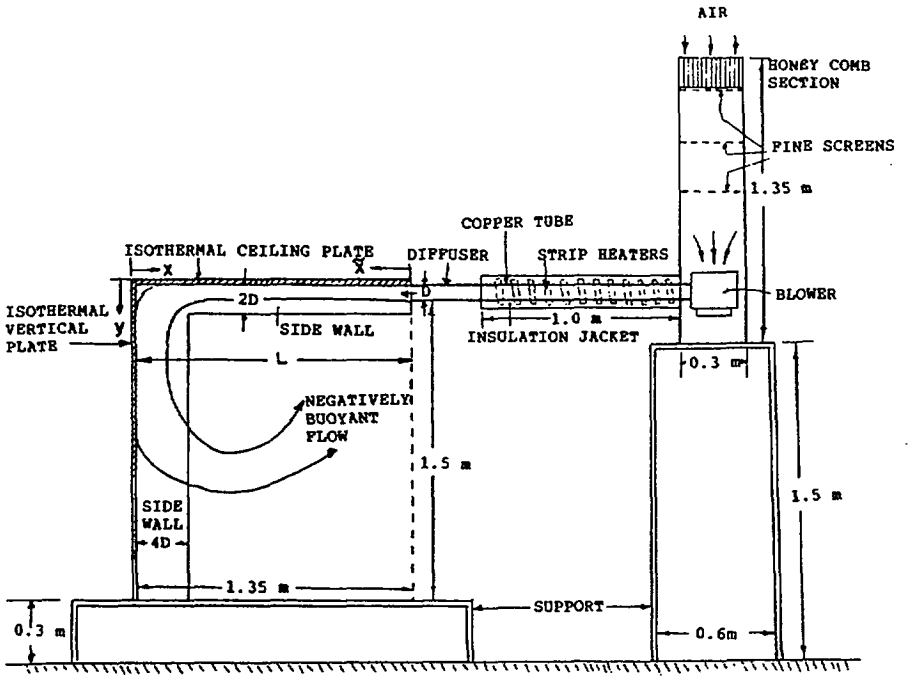

Fig. 1 Experimental arrangement and coordinate system for the study of a heated, two-dimensional ceiling jet discharged horizontally and turning downward at a corner with a vertical surface

heat transfer characteristics of a downward-turning horizontal buoyant ceiling jet or at the flow near a corner. In this paper, an experimental study is carried out on this flow circumstance.

Experimental System

Figure 1 shows a sketch of the experimental arrangement employed for the study of a downward-turning heated, two-dimensional, horizontal ceiling jet in an isothermal medium. The coordinate system used is also shown. A blower is installed at the bottom of a vertical channel, which is 1.35 m high, 0.3 m × 0.3 m in cross section, and placed on a metal frame. A honeycomb section and three very fine screens are employed at the entrance to the channel. Two very fine screens, which are 0.3 m apart, are located in the middle portion of the channel. This arrangement gives rise to a very low level of turbulence (with the measured intensities less than about 0.5 percent) and a fairly uniform flow across the channel (with a variation in the dimensionless velocity of less than ±3 percent of the mean value). The blower sends ambient air, over a wide range of flow rates, through a heated copper tube. The copper tube is 5

Nomenclature

A_0 = cross-sectional area of the slot through which the heated air jet is discharged
C_p = specific heat of the fluid at constant pressure
D = height of the slot for jet discharge
g = magnitude of gravitational acceleration
Gr = Grashof number = $g\beta \times (T_0 - T_\infty)D^3/\nu^2$
h = local heat transfer coefficient = $q/(T_0 - T_s)$
k = thermal conductivity of air
L = horizontal distance between ceiling jet discharge and corner
$\dot{m}$ = mass flow rate
$\dot{m}_{in}$ = mass flow rate at jet discharge
Nu_D, $\overline{Nu}_D$ = local and average Nusselt numbers, respectively, based on D
q = local heat transfer flux to the surface
Q = total net heat transfer to the isothermal surface from the heated jet flow
Q_{in} = total thermal energy input by the ceiling jet = $\rho_0 U_0 A_0 C_p \times (T_0 - T_\infty)$
Re = Reynolds number = $U_0 D/\nu$
Ri = Richardson number = Gr/Re^2
T = local temperature
U_0 = discharge velocity of the ceiling jet
u, v = horizontal and vertical velocity components, respectively
u^*, v^* = dimensionless horizontal and vertical velocity components, respectively, $u^* = u/U_0$, $v^* = v/U_0$
W = width of the horizontal and vertical plates
x = horizontal coordinate distance, measured from the vertical surface
$\bar{x}$ = distance along the two surfaces from the slot, around the corner
y = vertical coordinate distance measured downward from the horizontal surface
z = transverse coordinate distance
β = coefficient of thermal expansion of fluid
δ_p = penetration distance of jet flow, measured downward from horizontal surface
θ = dimensionless temperature = $(T - T_\infty)/(T_0 - T_\infty)$
ν = kinematic viscosity of fluid
ρ = density of fluid

Subscripts

0 = at jet discharge
∞ = ambient medium

cm in diameter and 1 m in length. It is heated by means of three fiberglass insulated heaters, which are wrapped around it. The energy input to each of the heaters is varied by means of individual power controllers. A diffuser at the end of the copper tube is employed to discharge the heated air as a two-dimensional jet, whose height could be varied. Several diffuser designs were considered to ensure uniform two-dimensional flow at the entrance. The heat loss from the copper tube and the diffuser to the environment was minimized by employing an insulated jacket, which has an inner layer of fiber glass and an outer layer of glass wool.

The discharge velocity of the jet U_0 could be varied from about 0.3 m/s to 2.5 m/s and the discharge temperature T_0 from room temperature to about 150°C. Thus, the arrangement could be used for studying fairly wide ranges of the governing parameters, which are the Reynolds number Re and the Grashof number Gr, both being based on the inlet conditions and defined later. The values for Re and Gr employed in the present experiments range from 2000 to 4000 and 0 to 10^6, respectively. The discharge velocity of the jet was determined by measuring the velocity distribution at the jet discharge and taking the average value. A calibrated DANTEC constant-temperature hot-wire anemometer was used, with the sensor positioned horizontally and normal to the x-axis. The hot wire was calibrated using a special calibration facility, designed for velocity levels in the range 0–0.5 m/s and for arbitrary flow direction (Tewari and Jaluria, 1990). Flow visualization was also carried out with smoke to confirm the results interpreted from temperature and velocity data. Though not shown here for conciseness, visualization results supported the trends indicated by the local measurements.

The discharge temperature of the jet was measured by using a rake of five thermocouples, located across the jet discharge slot. The average of the five temperatures measured was taken as the jet discharge temperature T_0. Again, the discharge temperature was found to be fairly uniform, within ±2°C across the slot cross section, giving a variation of less than ±3 percent of the mean values considered in this study.

The heated, two-dimensional air jet is discharged horizontally into a flow region 1.5 m high and 1.35 m × 0.3 m in cross section; see Fig. 1. At the top of the region, a water-cooled aluminum plate, 1.25 cm thick, which represents the ceiling of the enclosure, is attached. Another water-cooled aluminum plate is located vertically on one side, thus forming a 90 deg corner with the ceiling plate. The two-dimensional diffuser is placed horizontally, adjacent to the ceiling plate, as shown in Fig. 1. The horizontal distance L between the corner and the jet discharge location can be varied from about 0.60 m to 0.95 m by moving the jet discharge slot along the ceiling plate. Isothermal conditions are used at the boundaries to simulate the initially cold walls at the early stages of a room fire.

The sides of the enclosure are kept partially open to ensure that the enclosure is not stratified. However, it is necessary to minimize edge flows in order to maintain the two dimensionality of the flow. Extensive experimental data were taken without any side walls and it was found that the discharged jet flow was largely confined to regions near the ceiling and the vertical wall. The velocity and temperature measurements suggested that the jet flow was confined to a maximum value of 2D from the ceiling and of 4D from the vertical wall. Based on these experimental observations, sidewalls of width 2D and 4D were used for the ceiling and the vertical wall, respectively. However, it was ascertained that the measurements near the midplane were largely unaffected by the presence of side walls. The bottom was kept open to allow entrainment from below and the vertical dimension of the tank was large enough to avoid any significant effect on the flow due to this open boundary.

The water-cooled ceiling and vertical plates have the same design. Four rectangular copper tubes, each 2.5 cm × 1.25 cm in cross section, run along the length of the plate. Water from an outside source enters at the top of the vertical plate and the water coming out from this plate is allowed to enter at one end of the ceiling plate and the water coming out at the other end of the ceiling plate is allowed to drain into a sink. The temperature of the water entering the plate is maintained at a desired value by mixing hot and cold water streams from two separate sources. Twelve thermocouples were embedded in the plate close to the surface to monitor the temperature. For further details of the plate assembly, see Kapoor and Jaluria (1989). The maximum dimensionless temperature difference measured between any two embedded thermocouples on the two plates was found to be less than 5 percent of the mean values in most cases.

The heat transfer from the hot jet to the ceiling and vertical plate was measured by means of microfoil heat flow sensors (RdF type 20472-3) flush with the surface. Each heat flow sensor was 15 mm × 6 mm in surface area and 0.3 mm in thickness, and could be attached easily to the plate surface. The typical distance between two heat flux sensors along the ceiling and vertical plate was approximately 5.0 cm except near the corner where the sensors were placed 1 cm from each other. It was ensured that the heat flux gages did not significantly affect the local temperature and heat flux by estimating the additional thermal resistance introduced and by comparison with independent measurements of these quantities. The electric output (in millivolts) from the heat flux sensor was converted into heat flux (in W/m^2) with the help of individual calibration curves supplied by the manufacturer and verified in the laboratory by employing surfaces with known heat flux inputs. The accuracy of the measured heat flux was estimated to be high, with an estimated error of less than 5 percent in the present experiments. The outputs of the heat flux sensors were constantly monitored on a strip chart recorder and all the heat flux data were collected by using a Keithley data acquisition system. Thus, the errors in the reported Nusselt and Richardson numbers were estimated to be less than 5 and 3 percent, respectively. Considerable care had to be exercised to obtain accurate and repeatable data. In general, the repeatability was very high, being within 5 percent of the measured values for most measurements reported here.

Results and Discussion

The height D of the two-dimensional slot through which the hot jet is discharged is taken as the characteristic dimension in order to quantify the inlet conditions of the flow, as discussed by Goldman and Jaluria (1986). Thus, the governing parameters are obtained as the Reynolds number Re and the Grashof number Gr. The Richardson number Ri = Gr/Re^2, which is also known as the mixed convection parameter, is frequently employed in the literature to indicate the relative buoyancy level. These parameters, along with the Nusselt number Nu_D, which gives the dimensionless heat transfer rate, are defined as

$$\mathrm{Re} = \frac{U_0 D}{\nu}, \quad \mathrm{Gr} = \frac{g\beta(T_0 - T_\infty)D^3}{\nu^2} \tag{1}$$

$$\mathrm{Ri} = \frac{\mathrm{Gr}}{\mathrm{Re}^2}, \quad \mathrm{Nu}_D = \frac{hD}{k} \tag{2}$$

Also, the dimensionless velocities u^* and v^* and temperature θ are defined as

$$u^* = \frac{u}{U_0}, \quad v^* = \frac{v}{U_0}, \quad \theta = \frac{T - T_\infty}{T_0 - T_\infty} \tag{3}$$

All the symbols are defined in the nomenclature. It has been shown in several earlier papers, mentioned here, that the dominant parameter in these flows is the Richardson number Ri and, even though the Reynolds number Re is obviously important in characterizing the flow, particularly near the boundaries, the results are well correlated in terms of Ri alone. The effect of Re, over the range considered in the experiments, was indeed

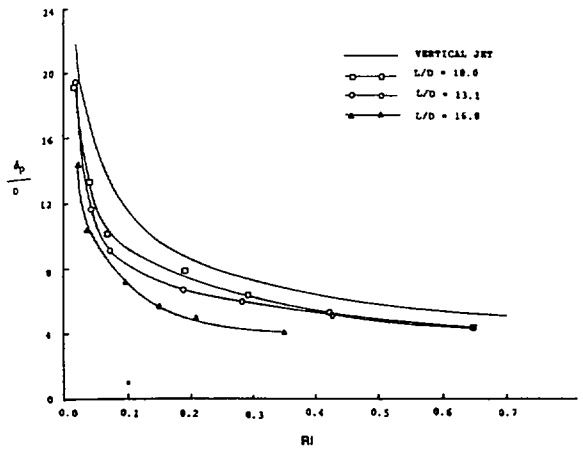

Fig. 2 Variation of the penetration depth δ_p with Ri at various values of L/D

found to be small compared to that of Ri and, thus, the results are largely presented in terms of Ri and other variables arising from the geometry and the thermal conditions.

Downward Turning of the Ceiling Jet. The buoyant horizontal ceiling jet, after losing some of its momentum and thermal energy to the ceiling, reaches the corner and turns downward along the vertical wall and behaves like a negatively buoyant wall jet, a flow that has been studied in detail by Goldman and Jaluria (1986) and Kapoor and Jaluria (1989). The heated wall jet flow penetrates downward to a finite distance due to its buoyancy, then turns upward and finally flows out of the enclosure.

The penetration distance δ_p, which represents the penetration of the thermal effects in the flow, is quantitatively taken as the location where 99 percent of the temperature drop has occurred, i.e., $\theta = 0.01$, indicating negligible thermal effects beyond this point. It was repeatedly found that this location was fairly well defined, within 1–2 cm. Similar results have been found earlier by Goldman and Jaluria (1986) and Kapoor and Jaluria (1989), for vertical heated jets discharged downward adjacent to vertical surfaces. The variations of the penetration distance δ_p with the mixed convection parameter Ri for L/D = 10, 13.1, and 16.8 are shown in Fig. 2. In all the cases shown, the ceiling and the vertical wall temperatures are essentially the same and are kept close to the ambient temperature (within ±1.0°C). It is seen that the penetration distance decreases with an increase in the mixed convection parameter Ri. These results are similar to those of a negatively buoyant wall jet. The penetration distance is found to be smaller at higher values of L/D, for a constant value of Ri. It was found from the detailed boundary layer measurements close to the ceiling plate that the momentum level decreases at a faster rate than the thermal buoyancy along the horizontal plate as the flow approaches the corner. Hence, for larger values of L/D, the momentum at the corner is smaller, resulting in smaller penetration distance.

The variation of the nondimensional penetration distance δ_p/D with Ri was measured over the range $0.02 \le \text{Ri} \le 0.65$. These results may be expressed in terms of the following correlations:

$$\frac{\delta_p}{D} = 3.65(\text{Ri})^{-0.41}, \quad \text{for} \quad L/D = 10 \qquad (4a)$$

$$\frac{\delta_p}{D} = 3.51(\text{Ri})^{-0.41}, \quad \text{for} \quad L/D = 13.1 \qquad (4b)$$

$$\frac{\delta_p}{D} = 2.77(\text{Ri})^{-0.41}, \quad \text{for} \quad L/D = 16.5 \qquad (4c)$$

The corresponding correlation for a vertical negatively buoyant wall jet, as obtained by Kapoor and Jaluria (1989) and shown in Fig. 2, is

$$\frac{\delta_p}{D} = 4.45(\text{Ri})^{-0.41} \qquad (5)$$

These correlations were found to be very accurate, with the correlation coefficients larger than 0.99. It is interesting to note that the exponents obtained for all cases are the same. The multiplication constant for the ceiling jet depends on the distance L between the corner and the location of the jet discharge. An attempt was made to obtain a general correlating equation incorporating the effects of both L/D and Ri. The correlation thus obtained was

$$\frac{\delta_p}{D} = 13.07(L/D)^{-0.54}(\text{Ri})^{-0.41} \qquad (6)$$

However, this correlation equation was found to be not as accurate as the earlier ones, the correlation coefficient being about 0.9.

In order to understand the basic physics of the flow field, detailed measurements of the thermal field, across the enclosure, were carried out. Only a few typical results are presented here for brevity. The thermal field was mapped very closely by using a rake of thermocouples at the middle of the width (z direction) of the enclosure. From these extensive temperature measurements, the corresponding isotherms were determined by interpo-

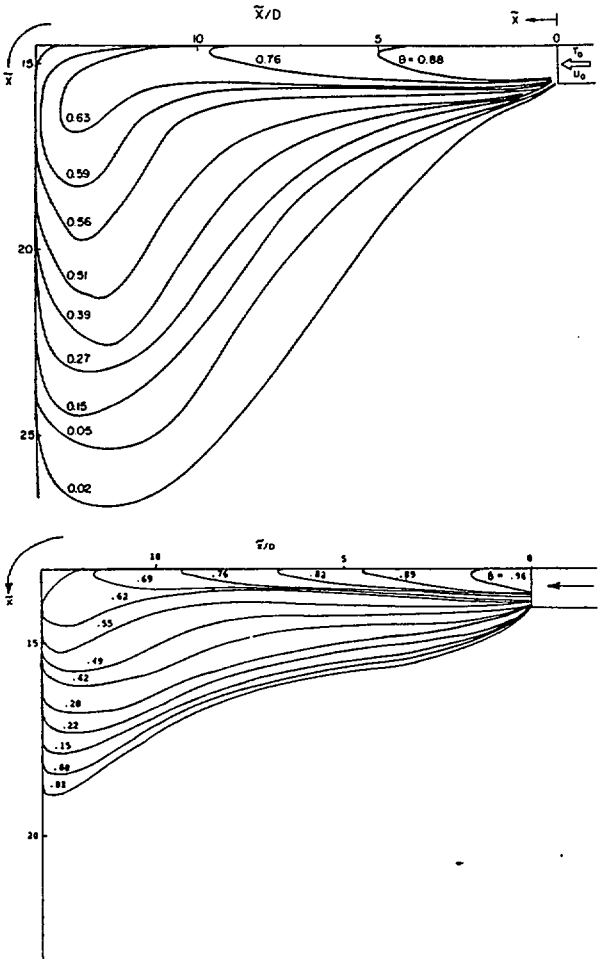

Fig. 3 Isotherms obtained from the temperature data at (*a*) Ri = 0.042 and (*b*) Ri = 0.303, for L/D = 13.1

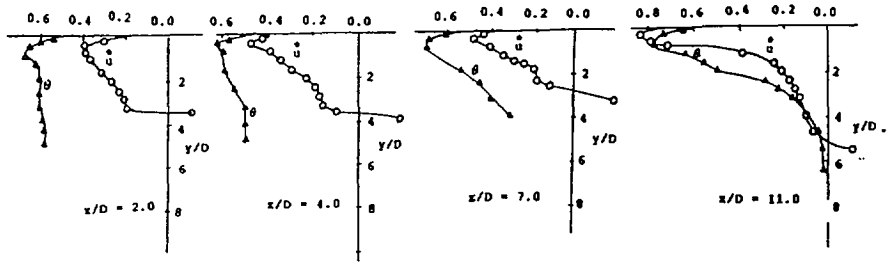

Fig. 4 Measured profiles of the horizontal component of the velocity and of the temperature near the ceiling at Ri = 0.043 and L/D = 13.1

lation. Figure 3 shows typical sets of such isotherms at Ri = 0.042 and 0.303. It is seen from the figure that the horizontal jet loses thermal energy as it flows toward the corner and then turns downward along the vertical wall. The jet flow penetrates downward up to a finite distance δ_p, as discussed earlier, and then stagnates before rising vertically upward due to its buoyancy and finally escaping out of the enclosure. The downward penetration is much less at the larger Ri. It is seen from the isotherms that the horizontal jet flow starts turning downward some distance before the corner. This indicates that the jet flow separates from the ceiling before reaching the corner and reattaches to the vertical wall at a certain distance downstream from the corner. This shows the presence of a small recirculation zone in the corner. The flow separation at the corner is further confirmed by the corresponding velocity profiles and heat flux measurements at the ceiling and the vertical walls, as discussed later in this paper.

Characteristics of the Flow Along the Ceiling and the Vertical Wall. Velocity measurements were carried out near the horizontal and vertical surfaces to characterize the flow field before and after the mixed convection flow turns at the corner. A constant-temperature hot-wire anemometer was used for the velocity measurements. It was ensured that the disturbance to the local flow due to the probe was small. Both the horizontal and the vertical components of velocity were measured. To measure the horizontal component u, the hot-wire sensor was kept vertical along the y direction, so that in the present two-dimensional flow, essentially the horizontal component of the flow velocity is measured. The vertical component v is measured by keeping the hot-wire sensor horizontal along the x direction so that essentially the vertical component of the flow velocity is measured (Jaluria, 1980).

Figure 4 shows the typical horizontal velocity and temperature distributions near the horizontal boundary at four stations between the jet discharge and the corner. It is seen from this figure that the velocity field decreases in both magnitude and thickness as the flow approaches the corner. However, as mentioned in the last section, the thermal field remains almost unchanged. It shows that the ceiling jet flow loses a significant amount of its momentum, but retains much of its thermal energy, as it moves toward the corner. It is interesting to observe from the figure that the slope of the velocity profile near the ceiling gradually decreases and becomes quite sharp near the corner (see Fig. 4(d)). This confirms the tendency of the jet flow to separate near the corner, as discussed in the last section. The jet flow reattaches to the vertical wall at a certain distance below the corner as seen in the next figure.

Figure 5 is the continuation of the flow described by Fig. 4 and shows the vertical velocity and temperature distributions near the vertical wall at four stations. It is seen from this figure that the magnitude and outward spread of the vertical velocity decrease as the jet flow penetrates downward. As expected, this trend is similar to the velocity and temperature fields obtained in the case of the penetration of a negatively buoyant vertical wall jet in an isothermal medium (Goldman and Jaluria, 1986) and in a thermally stratified medium (Kapoor and Jaluria, 1993). It is also seen from this figure that the velocity field decreases more rapidly than its temperature level. The slope of the velocity profile at the wall also decreases as the jet flow penetrates downward along the vertical wall. As mentioned ear-

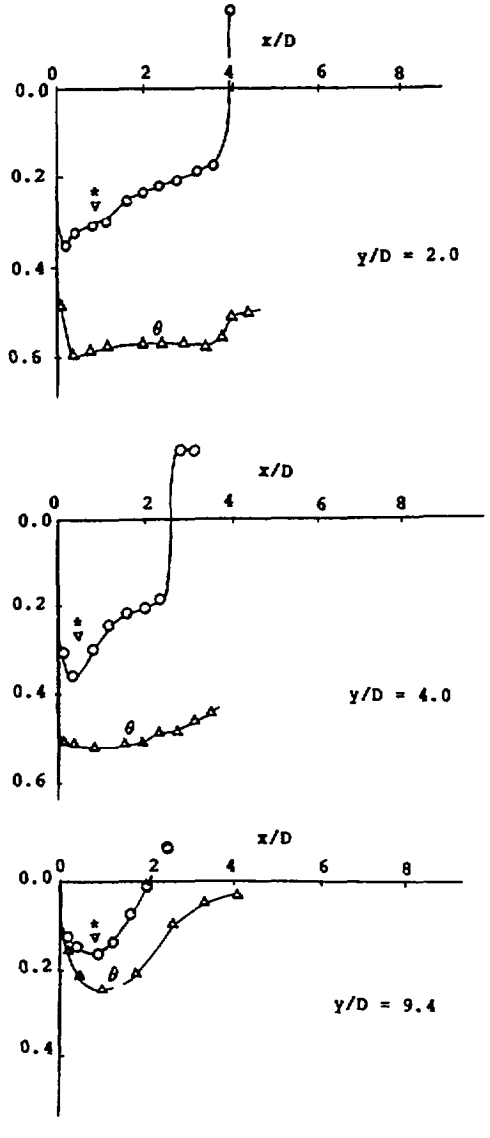

Fig. 5 Measured vertical velocity and temperature profiles near the vertical wall at Ri = 0.043 and L/D = 13.1

lier, this trend confirms the flow reattachment to the vertical wall at a certain distance below the corner. Also, as shown in Fig. 5(*a*), the jet flow tries to separate from the wall before becoming stagnant and then rising upward due to buoyancy, yielding a finite penetration distance δ_p.

From Figs. 4 and 5, the local mass flow rate can be obtained by integrating the corresponding product of the velocity and the density (as obtained from the measured temperature distributions) over the flow region. The mass flow rate $\dot{m}$ is nondimensionalized with the corresponding jet discharge mass flow rate $\dot{m}_{in}$. The variation of $\dot{m}/\dot{m}_{in}$ along the ceiling and the vertical wall for Ri = 0.0435 is shown in Fig. 6. It is seen from this figure that the ceiling jet entrains a significant amount of fluid from the surroundings as it flows along the ceiling wall. The mass flow rate first increases and then gradually decreases as the jet flow moves along the ceiling plate. After crossing approximately half of the length of ceiling plate, the flow rate remains almost constant over the rest of the boundary. This is an expected behavior for strongly stratified flows, for which the entrainment drops to zero as the local Richardson number becomes larger than about 1.0 (Koh, 1971). It is also seen from the figure that the mass flow rate remains almost constant as the flow turns downward at the corner. The flow rate gradually decreases along the vertical wall and finally becomes zero at the penetration distance. The corresponding penetration distance δ_p has also been shown in the figure. These results thus indicate the basic nature of such a downward-turning ceiling jet, of the resulting negatively buoyant wall flow, and of the flow in the neighborhood of the corner.

Net Mass Flow Entrainment by the Flow. As mentioned earlier, the negatively buoyant vertical wall jet entrains a significant amount of air from its surroundings (Goldman and Jaluria, 1986; Jaluria and Kapoor, 1988). The net mass flow entrainment was found to be dependent on the value of Ri of the discharged jet. It was found that the entrainment increases with an increase in Ri up to a value of around 0.4 and then it becomes almost constant in the range of $0.4 \leq \text{Ri} \leq 0.5$. These trends are due to decreasing δ_p and increasing vigor of the buoyancy-driven flow as Ri increases. The mass flow rate was obtained at different locations within the jet flow. Figure 7 shows the net flow rate near the horizontal surface at a distance of 4D from the corner for L/D = 10, 13.1, and 16.5. This flow rate is called $\dot{m}_1$ in the present experiments and is nondimensionalized with the corresponding discharge jet flow rate $\dot{m}_{in}$. It is seen from the figure that the ceiling jet entrains a significant amount of air up to a Ri value of around 0.2. The entrained mass flow was found to be higher at higher values of L/D. This is expected since a larger value of L/D implies greater length of the ceiling at constant D. This permits more surrounding air to be entrained by the ceiling jet. However, at higher values of Ri, there is very little flow entrainment into the ceiling jet flow,

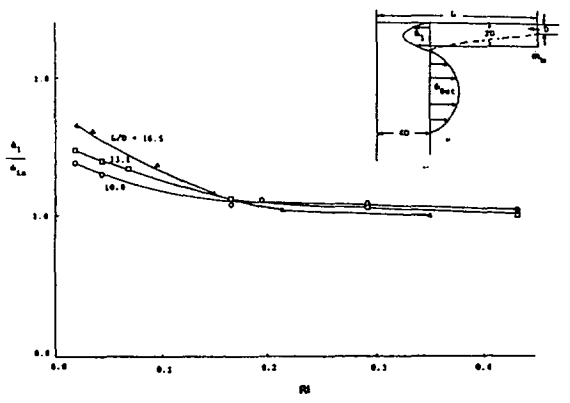

Fig. 7 Variation of the mass flow rate in the ceiling jet $\dot{m}_1/\dot{m}_{in}$ with Ri at different values of L/D

as mentioned above. In some cases, the mass flow rate was also measured at a distance of 2D below the corner near the vertical wall and it was found that this mass flow rate was almost the same as the corresponding mass flow $\dot{m}_1$. This suggests that the jet flow essentially does not entrain fluid while turning downward at the corner.

The net mass flow rate, $\dot{m}_{out}$ leaving the vertical flow region was measured at a distance of 4D from the vertical wall, using the corresponding horizontal velocity and temperature profiles. This mass flow rate represents the total entrainment into the downward turning ceiling jet, i.e., the sum of the mass flow entrained by the ceiling and the vertical wall flows, from the surroundings. Figure 8 shows the variation of $\dot{m}_{out}/\dot{m}_{in}$ with Ri. It is seen from this figure that the wall jet flow entails a significant amount of fluid after turning at the corner. As discussed earlier, the jet flow rate remains almost constant during the turn at the corner and most of the fluid is entrained when the jet flow penetrates downward along the vertical wall and when it rises upward due to buoyancy. It is seen from this figure that the entrained mass flow decreases with an increase in Ri. This is again an expected result because at a higher value of Ri, the flow penetration is decreased, resulting in smaller flow entrainment. These trends are similar to those found in the earlier investigations by Goldman and Jaluria (1986) and Jaluria and Kapoor (1988) for a negatively buoyant vertical wall jet. It is seen from Fig. 8 that the entrainment is smaller for a larger value of L/D. This is due to the fact that, in case of a larger L/D, the

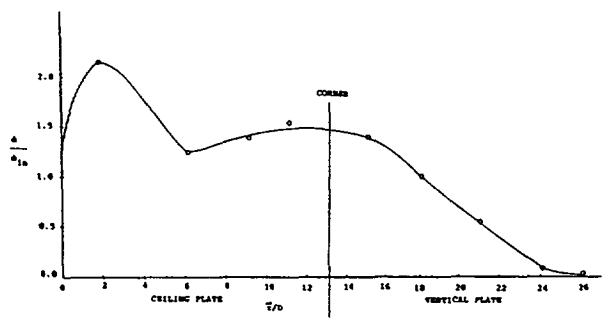

Fig. 6 The variation of the mass flow rate in the ceiling and the wall jets with distance $\bar{x}$ from the slot along the two surfaces at Ri = 0.043 and L/D = 13.1

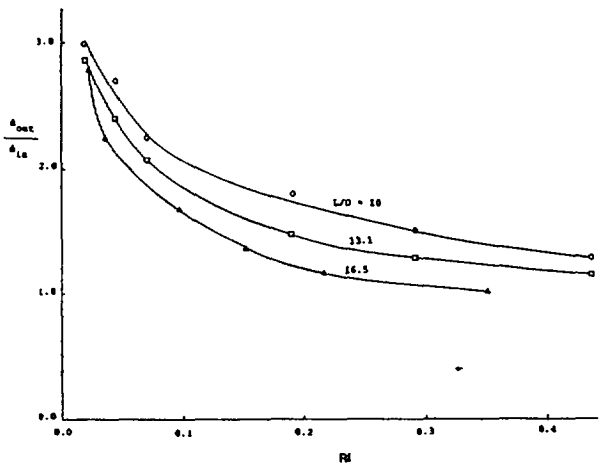

Fig. 8 Variation of the dimensionless total mass flow rate $\dot{m}_{out}/\dot{m}_{in}$ with Ri at different values of L/D

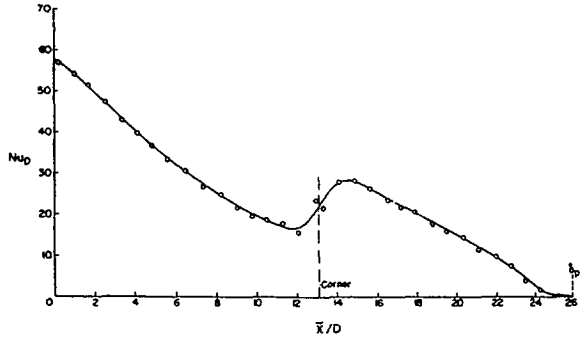

Fig. 9 Variation of the local Nusselt number Nu_D with distance $\bar{x}$ from the slot along the two surfaces at Ri = 0.042 and L/D = 13.1

penetration distance δ_p is smaller, as discussed earlier, resulting in smaller fluid entrainment.

Heat Transfer From the Ceiling Jet to the Isothermal Surfaces. Figure 9 shows the variation of the local Nusselt number Nu_D along the horizontal and the vertical plate at Ri = 0.042 and L/D = 13.1. It is seen that the local Nusselt number decreases along the ceiling and reaches its smallest value just before the corner. As the ceiling jet turns at the corner, the local heat transfer rate is seen to increase sharply downstream and to reach its maximum value just below the corner indicating the point of flow reattachment to the vertical wall. From this point, the heat transfer rate decreases gradually along the vertical wall and becomes almost zero at a location close to the penetration distance δ_p, which has also been shown in the figure. These results clearly show that a minimum and a maximum arise in the heat transfer rate on either side of the corner. This figure also confirms the earlier results that the flow separates from the horizontal plate before the corner and reattaches itself to the vertical wall just below the corner. All these results indicate the existence of a small recirculation zone in the corner.

Figure 10 shows the variation of the local Nusselt number Nu_D along the ceiling and the vertical plate for four values of Ri and for L/D = 10. The basic trends are similar to those observed in Fig. 9. The dimensionless local heat transfer rates, in terms of the Nusselt number, are seen to be higher for the smaller values of Ri. It should be mentioned here that the measured value of local heat flux q is actually smaller at the lower value of Ri. Higher values of Nu_D are obtained because of still smaller value of $(T_0 - T_\infty)$. It is seen from the figure that, in general, the local heat transfer rate first decreases along the ceiling plate, then increases at the corner and again decreases along the vertical plate, becoming almost zero at some location downstream. The penetration distance δ_p has also been marked on the figure. The decrease in Nu_D along the ceiling and the wall is obviously due to the increasing boundary layer thickness of the flow (Jaluria, 1980).

It is seen in Fig. 10 that the recovery in the local heat transfer rate at the corner depends upon the value of Ri. The recovery in the local heat flux was found to be larger for the smaller values of Ri. At the lower value of Ri, the ceiling jet flow has relatively larger momentum before it turns downward at the corner. Therefore, it separates from the ceiling plate at a larger distance from the corner and reattaches itself to the vertical wall at a larger distance below the corner. This suggests that at the smaller value of Ri, the size of recirculation region at the corner is larger than that found at the higher values of Ri. Hence, at the smaller value of Ri, the separated ceiling jet flow has to travel a larger distance at the corner before it reattaches itself to the vertical wall, resulting in a higher heat transfer recovery factor.

The variation of the average Nusselt number $\overline{Nu}_D$ for the ceiling plate with Ri for L/D = 10, 13.1, and 16.5 is shown in Fig. 11. The total net heat transfer rate to the ceiling $Q_{ceiling}$ was obtained by integrating the measured heat flux over the length of the ceiling plate. It is seen from this figure that the average Nusselt number decreases with an increase in Ri. This is due to the fact that, while the net heat transfer to the ceiling plate $Q_{ceiling}$ increases with Ri, the jet temperature difference $(T_0 - T_\infty)$ increases more rapidly than $Q_{ceiling}$. This results in a lower average heat transfer coefficient and hence a lower value of $\overline{Nu}_D$ at higher Ri. Figure 11 shows that the average Nusselt number was also found to be larger for the lower value of L/D due to the average film thickness being lower.

The variation of the average Nusselt number $\overline{Nu}_D$ for the vertical plate was also obtained. The basic trends of the results were similar to those discussed in the case of the ceiling plate. The variation of the average Nusselt number $\overline{Nu}_D$ for both the ceiling and the vertical wall with Ri is shown in Fig. 12. The results show the average heat transfer rate from the jet flow to the ceiling and the vertical wall. The basic trends, as expected, are a combination of individual results for the ceiling and the vertical wall.

All these results may also be expressed in terms of correlating equations to indicate the dependence of $\overline{Nu}_D$ on Ri and L/D. There is also a weak additional dependence on Re. However, for such turbulent mixed convection flows, the dependence on Ri is found to be much stronger than that on either Gr or Re and the results may be expressed fairly accurately in terms of

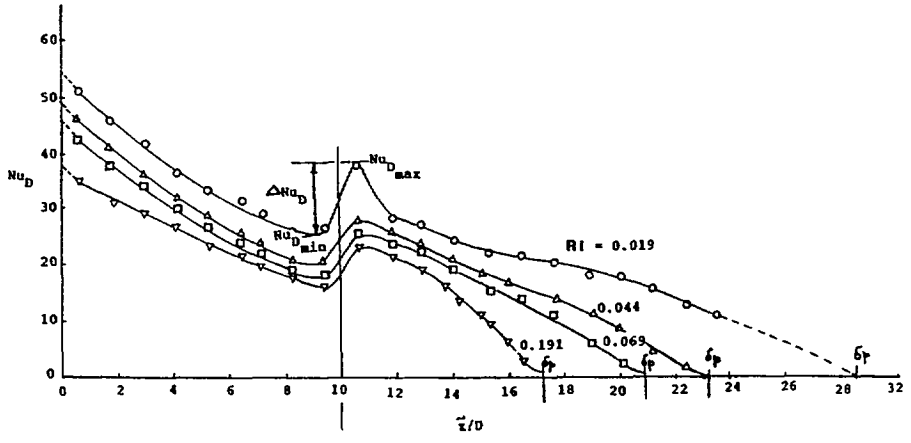

Fig. 10 Distribution of the local Nusselt number Nu_D over the ceiling and the vertical wall for Ri = 0.019, 0.044, 0.069, and 0.191 at L/D = 10.0

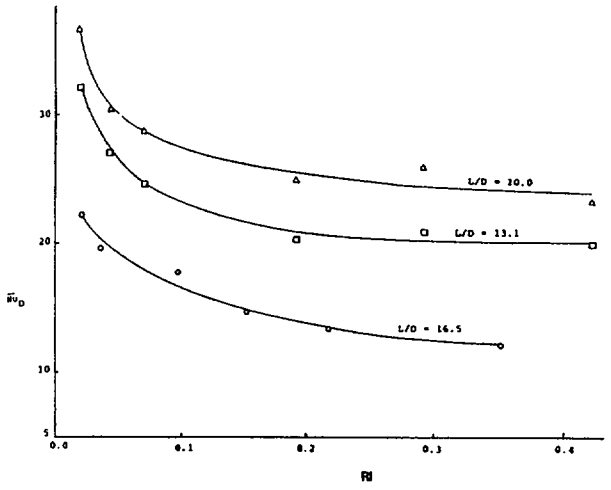

Fig. 11 Variation of the average Nusselt number $\overline{Nu}_D$ with Ri for the ceiling plate at different values of L/D

the mixed convection parameter. Thus, over the ranges $0.02 < Ri < 0.65$ and $10 < L/D < 20$, the experimental results are well correlated by the equations:

$$(\overline{Nu}_D)_{ceiling} = 250.47(Ri)^{-0.15}(L/D)^{-1.0} \quad (7)$$

$$(\overline{Nu}_D)_{wall} = 82.77(Ri)^{-0.25}(L/D)^{-0.8} \quad (8)$$

$$(\overline{Nu}_D)_{ceiling+wall} = 61.35(Ri)^{-0.09}(L/D)^{-0.5} \quad (9)$$

The correlation coefficients for these equations are larger than 0.95, indicating a fairly close approximation of the data with these equations.

Conclusions

A detailed experimental study has been carried out to investigate the basic flow characteristics of a heated horizontal ceiling jet, which turns downward at a corner. A heated two-dimensional jet is discharged horizontally adjacent to the underside of an isothermal horizontal surface in a large enclosure. An isothermal vertical plate was fixed at the other end of this surface, making a right angle corner. The following are the major findings of the present study:

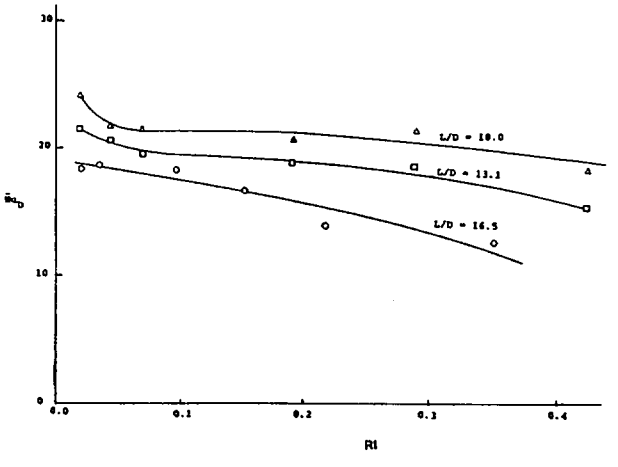

Fig. 12 Variation of the average Nusselt $\overline{Nu}_D$ with Ri for the total heat transfer to the ceiling and the vertical wall

1 The penetration distance δ_p was found to decrease with an increase in Ri. The penetration distance was also found to be smaller for higher values of L/D at a constant value of Ri. These trends are explained in terms of the underlying physical mechanisms and correlating equations for δ_p in terms of these parameters are derived from the data.

2 The detailed velocity and temperature measurements near the ceiling and the vertical wall show that the flow separates from the ceiling just before the corner and reattaches itself to the vertical wall at some distance below the corner.

3 The isotherms indicate the basic nature of the corner flow. The local heat flux measurements on the ceiling and vertical wall show that a minimum arises just before the turn and a recovery in the local heat transfer rate occurs after the turn due to reattachment of the flow.

4 The ceiling jet entrains some fluid from the surroundings as it flows along the ceiling. The flow rate remains almost unchanged as the flow turns at the corner. After turning at the corner, the flow again entrains a large amount of ambient air as it penetrates along the vertical wall and rises as an upward buoyant plume. This results in a large flow rate generated by the downward-turning ceiling jet. The net flow entrainment at different locations was obtained and correlated in terms of the mixed convection parameter Ri of the discharge jet. It was found that the overall net mass flow rate decreases with an increase in Ri.

5 The heat transfer recovery at the corner, i.e., the difference between the maximum and minimum Nu_D on either side of the corner, was found to decrease with the mixed convection parameter Ri of the discharged ceiling jet. This suggests that at a lower value of Ri, the jet flow separation from the ceiling and reattachment to the vertical wall occur at larger distances from the corner. This indicates that the size of the recirculation zone at the corner decreases with an increase in Ri of the discharged ceiling jet.

6 The average Nusselt number $\overline{Nu}_D$ for the ceiling and the vertical wall, put together, was found to decrease with Ri and to be smaller for a larger value of L/D at a constant Ri. These trends are explained in terms of the underlying physical mechanisms and the area over which heat transfer occurs.

Acknowledgments

This research was carried out with support from the Building and Fire Research Laboratory of the National Institute of Standards and Technology, United States Department of Commerce, under grant number 60NANB7D0743. The several interactions with Dr. L. Y. Cooper during the course of this work are also acknowledged.

References

Alpert, R. L., 1975, "Turbulent Ceiling Jet Induced by Large Scale Fires," *Combustion Science and Technology*, Vol. 11, pp. 197–213.

Baines, W. D., and Turner, J. S., 1969, "Turbulent Buoyant Convection From a Source in a Confined Region," *J. Fluid Mech.*, Vol. 37, pp. 51–80.

Baines, W. D., Turner, J. S., and Campbell, I. H., 1990, "Turbulent Fountains in an Open Chamber," *J. Fluid Mech.*, Vol. 212, pp. 557–592.

Chen, C. J., and Rodi, W. A., 1979, *Vertical Turbulent Buoyant Jets: A Review of Experimental Data*, Pergamon Press, Oxford, United Kingdom.

Cooper, L. Y., 1982, "Heat Transfer From a Buoyant Plume to an Unconfined Ceiling," ASME JOURNAL OF HEAT TRANSFER, Vol. 104, pp. 446–451.

Cooper, L. Y., 1989, "Heat Transfer in Compartment Fires Near Regions of Ceiling-Jet Impingement on a Wall," ASME JOURNAL OF HEAT TRANSFER, Vol. 111, pp. 455–460.

Goldman, D., and Jaluria, Y., 1986, "Effect of Opposing Buoyancy on the Flow in Free and Wall Jets," *J. Fluid Mech.*, Vol. 166, pp. 41–56.

Jaluria, Y., 1980, *Natural Convection and Mass Transfer*, Pergamon Press, Oxford, United Kingdom.

Jaluria, Y., 1986, "Hydrodynamics of Laminar Buoyant Jets," in: *Encyclopedia of Fluid Mechanics*, N. P. Chereminoff, ed., Gulf, Houston, TX, Vol. 2, pp. 317–348.

Jaluria, Y., and Kapoor, K., 1988, "Importance of Wall Flows at the Early Stages of Fire Growth in the Mathematical Modeling of Enclosure Fires," *Combustion Science and Technology*, Vol. 59, pp. 355–369.

Kapoor, K., and Jaluria, Y., 1989, "Heat Transfer From a Negatively Buoyant Wall Jet," *Int. J. Heat Mass Transfer*, Vol. 32, pp. 697–709.

Kapoor, K., and Jaluria, Y., 1993, "Penetrative Convection of a Plane Turbulent Wall Jet in a Two-Layer Thermally Stable Environment," *Int. J. Heat Mass Transfer*, Vol. 36, pp. 155–167.

Koh, R. C. Y., 1971, "Two-Dimensional Surface Warm Jets," *J. Hyd. Div.*, Vol. 97, pp. 819–836.

List, E. J., 1982, "Turbulent Jets and Plumes," *Ann. Rev. Fluid Mech.*, Vol. 14, pp. 189–212.

Morton, B. R., 1959, "Forced Plumes," *J. Fluid Mech.*, Vol. 5, pp. 151–163.

Motevalli, V., and Marks, C. H., 1990, "Transient and Steady State Study of Small-Scale Unconfined Ceiling Jets," in: *Heat and Mass Transfer in Fires*, J. G. Quintiere and L. Y. Cooper, eds., ASME HTD-Vol. 141, pp. 49–61.

Seban, R. A., Behnia, M. M., and Abreu, J. E., 1978, "Temperatures in a Heated Jet Discharged Downward," *Int. J. Heat Mass Transfer*, Vol. 21, pp. 1453–1458.

Tewari, S. S., and Jaluria, Y., 1990, "Calibration of Constant-Temperature Hot-Wire Anemometers for Very Low Velocities in Air," *Rev. Sci. Instrum.*, Vol. 61, pp. 3834–3845.

Turner, J. S., 1966, "Jets and Plumes With Negative or Reversing Buoyancy," *J. Fluid Mech.*, Vol. 26, pp. 779–792.

Turner, J. S., 1979, *Buoyancy Effects in Fluids*, Cambridge Univ. Press, Cambridge, United Kingdom.

Veldman, C. C., Kubota, T., and Zukoski, E. E., 1975, "An Experimental Investigation of Heat Transfer From a Buoyant Gas Plume to a Horizontal Ceiling—Part 1—Unobstructed Ceiling," National Bureau of Standards, Rep. No. NBS-GCR-77-97.

You, H. Z., 1985, "An Investigation of Fire-Plume Impingement on a Horizontal Ceiling: 2—Impingement and Ceiling Jet Regions," *Fire and Materials*, Vol. 9, pp. 46–55.